Received 15 August 2025; Accepted 12 January 2026
https://doi.org/10.48612/letters/2026-1-78-83
https://elibrary.ru/ktoxvt

Kinetics of self-healing of a main crack in WC-Co hard alloy

T. V. Kozlova†, I. N. Sevostyanova, A. G. Burlachenko, A. A. Neiman, S. P. Buyakova

†kozlovatv@ispms.ru

Institute of Strength Physics and Material Science, Russian Academy of Sciences, Tomsk 634055, Russia

Abstract: The paper studies the kinetics of self-healing of a main crack in tungsten carbide-cobalt (WC-8 mass % Co). The self-healing in WC-Co hard alloy occurs through the liquid-phase recovery with cobalt and partially dissolved tungsten carbide acting as healing agents. Over an eight-hour holding near the sintering temperature, the total crack length was reduced by 30%. The maximum crack width capable to self-healing through the liquid-phase recovery was approximately 50 μm. One-hour healing led to filling of the crack zone with cobalt. Further self-healing resulted in the growth of individual grains into binder in the healed zone. Six-hour isothermal holding near the sintering temperature resulted in elimination of the differences in the microstructure between the healed area and the base material, however, a significant cobalt depletion and the formation of brittle η-phase (Co_3W_3C or Co_6W_6C) indicating a decrease in the carbon content made further self-healing processes impossible. As self-healing mechanism is limited by healing agent content in WC-Co alloys, large damages elimination requires the use of external healing agents. For the practical solution of the extensive defects recovery, it was proposed to use hetero-healing methods, for example, isothermal holding in a carburized atmosphere and the use of infiltrates based on WC-Co mixtures with cobalt excess.

Keywords: self-healing, WC-Co hard alloy, liquid phase healing, η-phase, healing agent

Acknowledgements: *The work was performed according to the Government research assignment for ISPMS SB RAS (FWRW-2026-0002).*

1. Introduction

Currently many studies are focused on increasing the service life and performance characteristics of engineering materials by restoring their lost integrity and original properties [1–4]. Among them, the self-healing mechanisms — the ability to autonomously repair defects without the use of external healing agents appears to be the most promising [4–7].

Modern self-healing methods can be divided into three main groups according to the acting mechanism [5,8]. The first method, which is based on chemical oxidation, is primarily used for ceramic materials. During the chemical reaction, the volume of oxidation products exceeds that of the original material, allowing them to effectively fill defects [5]. The oxide crack filling is typical mainly for binary ceramics like SiC and Si_3N_4, transition metals, binary intermetallic phases including aluminides, silicides, and borides [6]. The second self-healing method relies on phase transformations. This mechanism has been studied in detail in zirconium dioxide stabilized in the tetragonal phase [7,9]. The tetragonal-to-monoclinic phase transformation is accompanied by a local volume increase of 3–4%, which leads to compressive stresses that prevent crack propagation [9]. The third self-healing method involves mechanisms of high-temperature diffusion and mass transfer, which have been observed in both ceramics and metals, as well as hard alloys [5,8,10].

In metallic alloys self-healing can occur by diffusion due to the segregation of the most mobile atoms into a defect [10]. The chemical composition of such alloys is generally similar to that of the commercial alloys and the healing agent cannot be identified as a separate phase in the microstructure but present as an alloying element in a supersaturated state. However, high diffusion capacity of the alloying component is not the only requirement for self-healing. In many cases damage healing requires a solid-state reaction that results in the formation of a new phase with an average atomic volume significantly higher than that of its constituent atoms [10]. A similar healing mechanism was studied on austenitic steels during creep [11]. It was found that adding boron and nitrogen to austenitic stainless steels leads to effective healing of creep cavities because BN phase formed under creep conditions and are predominantly deposited on the free surfaces of cavities [11]. To identify the mechanism and criteria for self-healing during creep, a number of binary systems Fe-Cu, Fe-Au, Fe-Mo and Fe-W were studied as model alloys [12].

However, among diffusion methods, heating to the melting point of the alloy component with lower T_m is the most effective and practically used method for healing defects. [10,13]. It that case the lower T_m component serves as the healing agent, while the second/other components remain as a solid matrix. The liquid-phase healing agent penetrates the defect partially or completely fills it and then crystallizes. If the alloy composition remains unchanged, self-healing can occur multiple times throughout the entire service life.

Although the liquid-phase healing mechanism has significant advantages, including fast healing kinetics,

there is one functional limitation related to the maximum acceptable defect size. Large-scale damage can lead to weakening of capillary forces and thus to incomplete healing [1]. An alternative to liquid-phase self-healing is increasing the amount of healing agent; however, this may change the mechanical properties of the material.

Alloys with eutectic compositions are of significant importance among materials capable of liquid-phase healing. Under melting point (T_m) these alloys undergo dissolution not only of the lower T_m component but also partial dissolution of the solid matrix. Further crystallization under cooling helps eliminate differences in composition and structure between the healed defect and the base material. Among them, tungsten carbide-based alloys with cobalt (WC-Co) and nickel (WC-Ni) binder are one of the most widely used materials.

The problem of liquid-phase healing of hard alloys based on tungsten carbide has not been sufficiently covered in the literature. The first attempts to heal microcracks formed by indentation in WC-Co hard alloy were undertaken in the work of S. B. Luyckx and W. Barlow-Jones [13]. It was shown that short-term annealing of WC-Co samples in the temperature range of 600 – 800°C leads to only partial healing of microcracks [13]. Considering WC-Co alloys have wide industrial application due to high strength characteristics, wear resistance and acceptable plasticity, the study of the self-healing kinetics of defects formed during service is an urgent task.

2. Materials and methods

The sample was cut from a WC-8 mass % Co sealing ring with a through crack. The average grain sizes of the carbide and binder before healing were d_{WC} = 1.7 ± 0.2 μm and d_{Co} = 0.9 ± 0.2 μm, respectively (Fig. 1). Cobalt volume fraction estimated by measuring the Co area at Scanning Electron Microscopy (SEM) images using the ImageJ software was 16.4%.

The sample was repeatedly heated near the sintering temperature T_s = 1400°C with a holding at the maximum temperature for 1 – 2 hours in a vacuum furnace SNVE-1.3.1/16I3-UKHLCH.1 with a residual pressure of no higher than 10^{-3} mm Hg according to the mode shown in Fig. 2. Parameters of healing cycles are presented in Table 1.

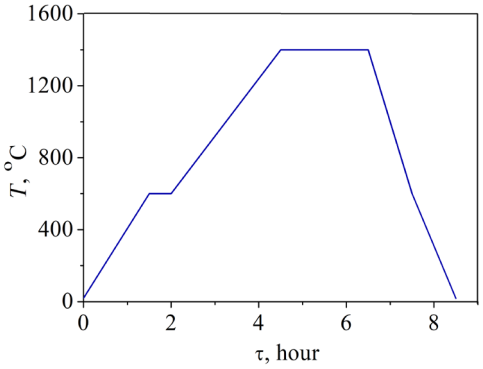

Fig. 2. Crack healing mode.

Table 1. Crack healing cycles.

N	1	2	3	4	5	6
Holding time at 1400° C, h	1	1	1	1	2	2
Total time, h	1	2	3	4	6	8

The weight and geometric characteristics of the sample were measured after each healing cycle. The sample was ground and polished using diamond pastes of different granularities. After polishing the sample was cleaned in isopropyl for 3 – 5 minutes using a VU-09 ultrasonic bath. η-phase was revealed by selective etching in as-prepared 20% equal volumes water solution of NaOH and $K_3[Fe(CN)_6]$ at 18 – 20°C for 2 – 3 seconds. The microstructure was studied using optical microscopy (Altami Met M1) and Scanning Electron Microscopy (SEM) (Tescan Vega 3). The volume fraction and grain sizes were estimated using the ImageJ software.

3. Results

The total length of the healed area at the edges of the sample was measured after each healing cycle (Fig. 3). The change in crack width (crack narrowing) was estimated in three areas marked with white frames in Fig. 3 a.

Figure 3 a shows that one-hour holding led to healing of the crack edges in area I, while in the central part of the sample, near the crack bending zone (area III), the distance between the crack faces remained large. A three-hour hold

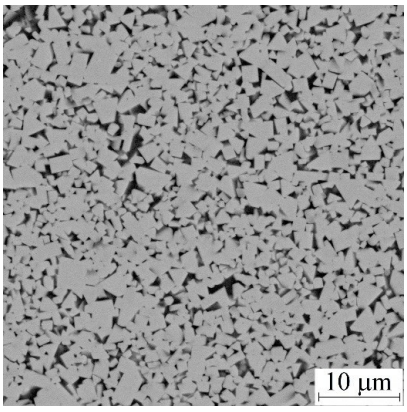

a

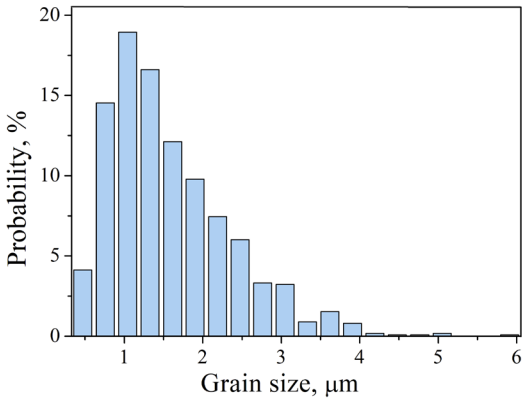

b

Fig. 1. SEM image of WC-Co sample before healing (a); WC grain size distribution (b).

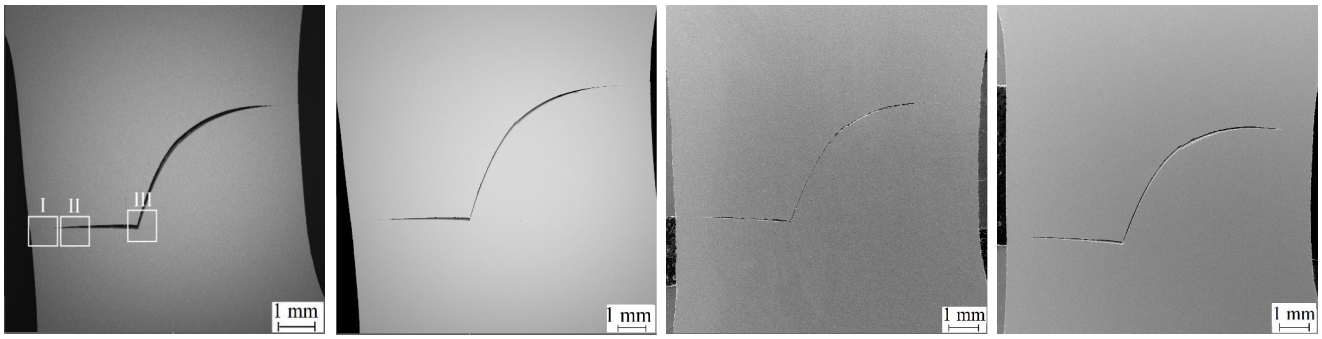

a b c d

Fig. 3. SEM images of a crack zone after one (a), three (b), six (c) and eight-hour holdings (d).

resulted in a significant reduction of the crack and an increase in the overall healing length (Fig. 3 b). A further increase in holding time (Fig. 3 c) caused the sample to shrink by 2.5%, accompanied by a noticeable tightening of the crack. After 8 hours of healing, the sample shrank by an additional 1%, and the total healing length increased significantly (Fig. 3 d). However, in the bending area III, the crack width became larger.

Figure 4 shows the dependence of the total healing length (a) and the width of the crack in three selected areas (b) on the holding time. The rate of healing varies depending on the holding time. Initially, the rapid recovery of the material at the crack edges occurs with the total healing length increasing by 14.3%. Further holding for up to 6 hours

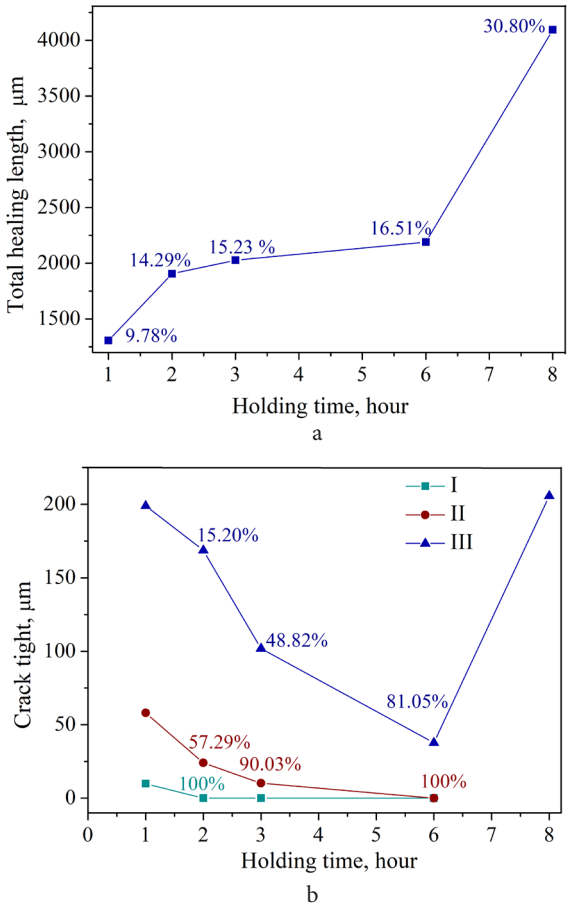

Fig. 4. (Color online) Kinetics of a crack healing in the WC-Co alloy — the dependence of the total healing length (a) and the width of the crack in three selected areas (b) on the holding time.

results in only a 2% additional increase in healing length. Holding from 6 to 8 hours leads to a sharp increase in the healing rate. Thus, successive isothermal holdings near the sintering temperature for 8 hours resulted in a total reduction of the crack length by 30% (Fig. 4 a). The crack width in the three selected regions decreases almost linearly with increasing holding time (Fig. 4 b). At the edge of the sample in the area I, where the minimal crack width is $h = 5$ μm, full healing is observed after two hours of holding (Fig. 4 b). In the area II, with an initial crack width of $h = 60$ μm, the crack reduces to half its original width after two hours of healing, and complete healing of the crack occurs after 6 hours. A linear narrowing of the crack occurs in area III and reaches its maximum value after 6 hours; however, further holding leads to the reopening of the crack to its initial state (Fig. 4 b). The increase in the crack width in the area III is associated with the degradation of the material at the crack surface after 8 hours of healing.

Figure 5 shows SEM images of the area I after isothermal holding near the sintering temperature for one (a), three (b), six (c) and eight hours (d).

One-hour holding leads to filling the crack ends with cobalt (dark areas in Fig. 5 a). Densification of carbide grains and cobalt depletion are observed in the areas near the crack. The cobalt volume fraction estimated from SEM images near the healing zone decreases significantly compared to the initial value of 16.3% (Table 2). At a distance of approximately 30 μm from the crack, the cobalt volume fraction is higher and closer to the initial value of 14.3% (Table 2). After one hour of healing, the grain size near the crack — where the cobalt volume fraction is lower — decreases to d=1.45 μm compared to the initial state of the alloy. Further increase in the holding time to three hours leads to the growth of large carbide grains into the cobalt binder in the restored areas of the sample (indicated by arrows in Fig. 5 b). The volume

Table 2. Structural parameters of WC-Co sample after healing.

τ, h	near the crack, ±10 μm		at the distance from the crack, >30 μm	
	φ_{Co}, % ±1%	$\langle d \rangle_{WC}$, ±0.3 μm	φ_{Co}, % ±1%	$\langle d \rangle_{WC}$, ±0.3 μm
1	10.5	1.45	14.3	1.76
3	9.67	1.47	10.75	1.93
6	8.12	2.08	8.67	2.09
8	6.35	2.32	6.21	2.4

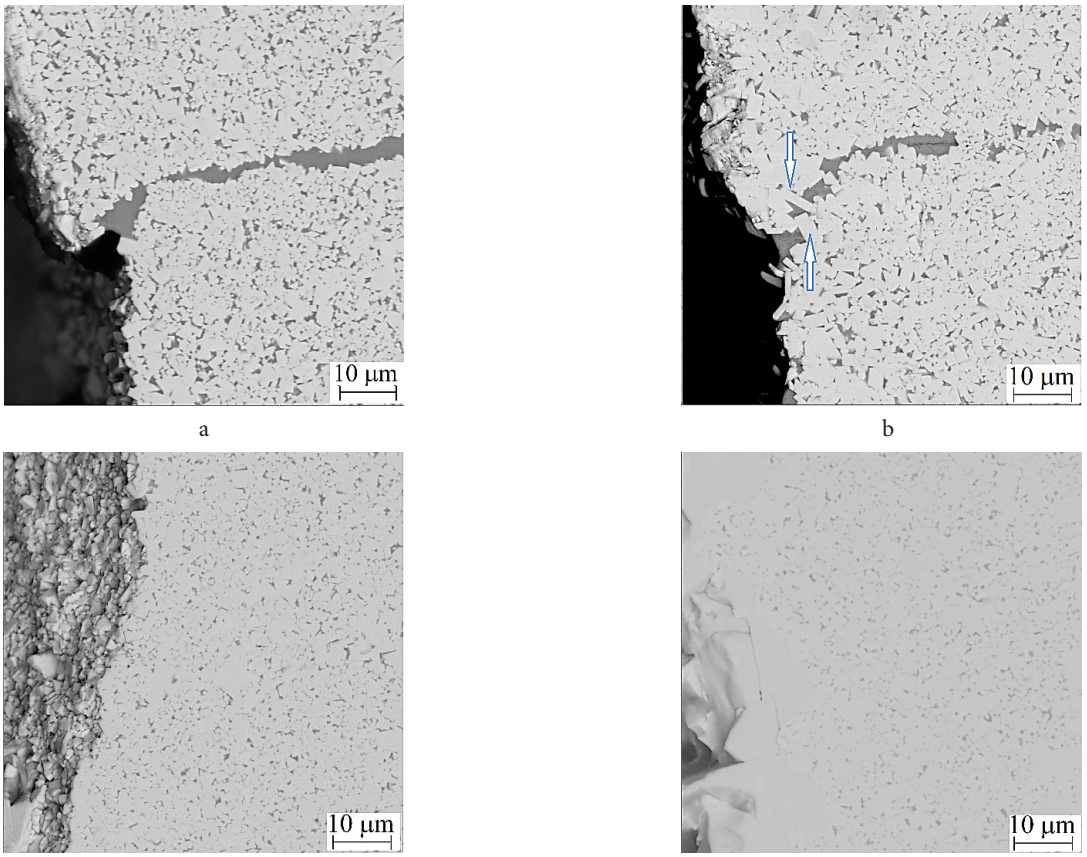

a b c d

Fig. 5. SEM images of the area I after one (a), three (b), six (c) and eight-hour holding (d).

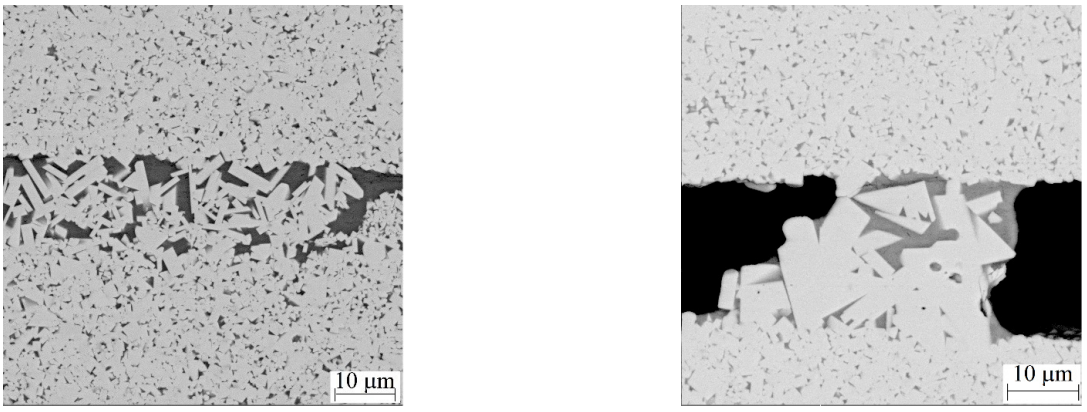

a b

Fig. 6. SEM images of the area II after three-hour holding.

fraction of cobalt decreases both near the crack and at a distance from it. A complete recovery of the material with a homogeneous dense structure is observed in the healed area after 6 hours of holding (Fig. 5 c). WC grains grow both near the crack and at a distance from it. Holding for 8 hours results in a further decrease in the cobalt volume fraction in the recovery area to approximately 6.3%, both near the former crack and at a distance from it.

Three-hour holding results in the formation of healing "bridges" in the area II, where the crack width is less than 20 μm (Fig. 6). According to [14], healing "bridges" are formed primarily on the protruding edges on the fracture surfaces. The size and morphology of WC grains in healing bridges differs from the morphology of the base material. In the healing bridges elongated platelet WC grains with well-defined morphology are observed within the cobalt binder, reaching sizes of up to d=10 μm (Fig. 6). In [14] it is shown that the nonequiaxial shape of WC grains in hard alloys is determined by the balance of shape relaxation and crystal growth processes. In this case, grain growth is determined by the higher volume fraction of cobalt in the healing bridges, whereas the relaxation process of the WC grain shape is independent of the surrounding matrix.

A six-hour isothermal holding resulted in the formation of a cobalt-rich layer along the crack with a width of up to 100 μm revealed by selective etching (Fig. 7a). Within this

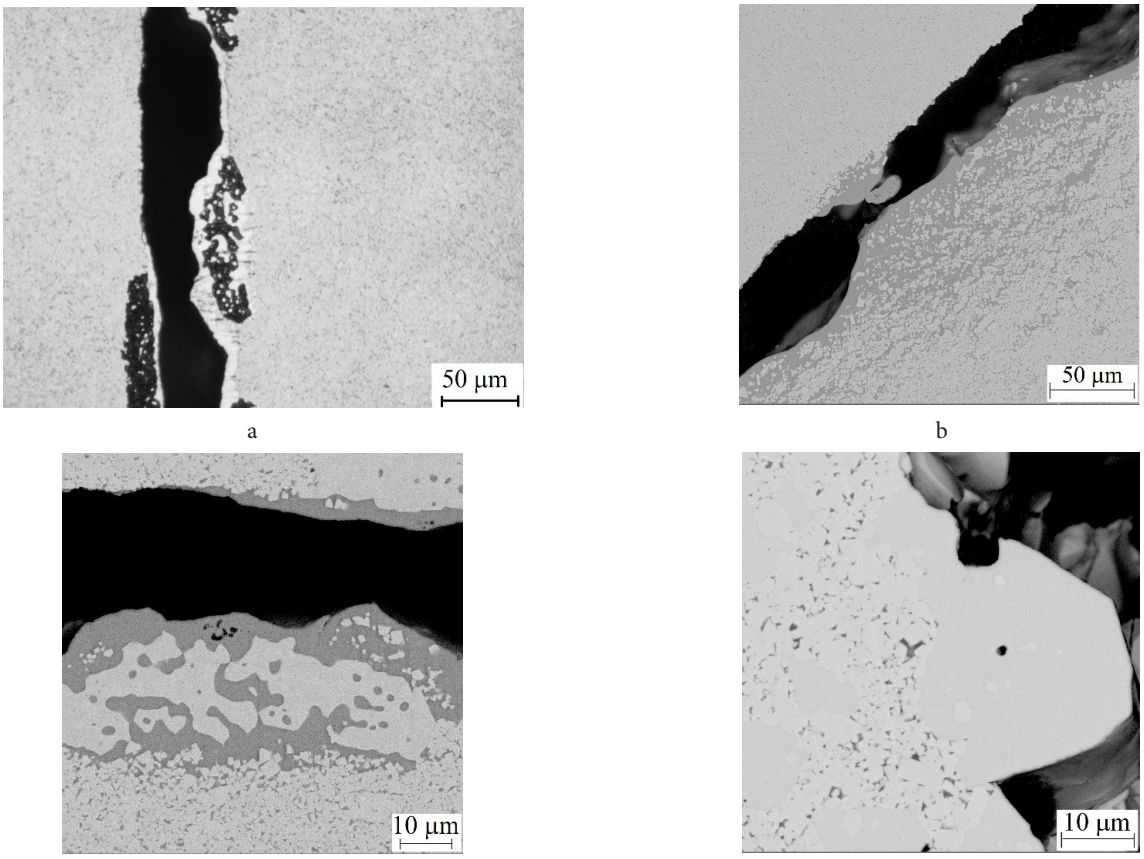

Fig. 7. Optical microscopy image of an etched surface in the crack zone (a); SEM images of a crack zone (b, c) and periphery of the sample (d) formed after six-hour holding.

layer, fine WC grains and localized regions of large η-phase grains are observed (Fig. 7b, c). The large η-phase grains are also visible at the edges of the specimen (Fig. 7d). The η-phase corresponds to a W-Co-C carbide, which forms under carbon-deficient conditions in the WC-Co system [15].

4. Discussion

The selected holding temperature T=1400°C corresponds to the melting point of the WC-Co eutectics. According to [16], when the T_m of the eutectic is reached, partial dissolution of tungsten carbide (up to 38%) in the cobalt binder occurs, followed by its crystallization. Thus, each isothermal holding near the sintering temperature leads to the formation of a healing agent — liquid cobalt with tungsten carbide dissolved in it, which crystallizes upon cooling, forming the structure of the hard alloy.

The SEM results show that after one hour of isothermal holding at T=1400°C, crack healing occurs by cobalt, which has a lower melting point. In this case, significant depletion of cobalt is observed in areas near the crack (Table 2). Cobalt migration to defects or additional free surfaces is driven by capillary phenomena during liquid flow, and the differences in capillary forces are determined by the varying sizes of Co channels between WC grains [16]. It follows that a smaller distance between WC grains or larger grain size results in a lower rate of liquid phase flow during healing.

The measurements taken near the healed area and at a distance from it indicate that the WC grain size is depended on the amount of liquid phase, or equivalently, by the tungsten carbide density in the surrounding binder; consequently, in regions close to the healed zone where cobalt content is lower than in the rest of the material, the grain size is smaller (Table 2). The change in the grain size and cobalt binder content in tungsten carbide-based hard alloys will affect the mechanical properties of the material [17–19].

After six hours of isothermal holding, the differences between the microstructure of the healed region and the surrounding material are eliminated, resulting in a uniform cobalt distribution and grain size both next to the healed area and at a distance from it (Fig. 5c, Table 2). However, significant changes in the structure of the sample are observed compared to the initial state. The volume fraction of cobalt decreases two times from the initial state (Table 2), and as cobalt is the main component of healing agent, its depletion leads to structure degradation and makes further self-healing impossible. Moreover, η-phase inclusions along the periphery of the sample and near the crack throughout its entire length (Fig. 7) indicates a loss of carbon during the healing process [15]. The η-phase itself is adverse, and the presence of large areas of brittle η-phase significantly degrades the mechanical properties of the hard alloy. The tendency of the η-phase to persist after cooling of the alloy indicates a high carbon deficiency. Although at a slight carbon deficiency, the η-phase is unstable and may decompose during cooling. Therefore, to achieve a desirable microstructure, samples containing η-phase are often subjected to additional sintering in a carburizing atmosphere [20].

Thus, consecutive isothermal holdings of the WC-Co sample with a main crack for eight hours resulted in healing of the crack in regions where its width does not exceed 50 μm by approximately 30%. In the restored areas, a homogeneous microstructure with denser carbide grains is formed. However, due to a significant depletion in cobalt and carbon content, the formation of microstructures unfavorable for mechanical properties occurs along with material degradation near the crack and at the periphery of the sample. This degradation makes further self-healing of the crack impossible. To completely eliminate large-scale damage in the hard alloy, it is necessary to employ hetero-healing methods such as sintering in a carburizing atmosphere and the use of WC-Co infiltrates through processing similar to binder jetting manufacturing [21,22].

5. Conclusions

This study examined the self-healing of a main crack in a WC-8 mass % Co alloy via liquid-phase healing near the sintering temperature. An analysis of the self-healing kinetics, combined with microstructure characteristics, led to the following conclusions:

1. Successive isothermal holdings of a WC-Co hard alloy sample near the sintering temperature for up to eight hours resulted in a 30% reduction in the length of the main crack.
2. The maximum crack width in a WC-Co hard alloy capable of self-healing is 50 μm and is determined by the amount of healing agent.
3. After six hours of isothermal treatment near the sintering, temperature differences in the microstructure between the healed area and the base material are eliminated.
4. The cobalt concentration is reduced by 50% following consecutive eight-hour isothermal holding near the sintering temperature. The formation of η-phase and material degradation at the sample edges and within the crack region indicate carbon depletion in the system. Further healing is only possible through external healing agents (carburizing atmosphere, infiltration with a eutectic WC-Co mixture).

References

1. S.K. Ghosh, ed., Self-Healing Materials: Fundamentals, Design Strategies, and Applications, 1st ed., Wiley, 2008.
2. A. La Monaca, J.W. Murray, Z. Liao, A. Speidel, J.A. Robles-Linares, D.A. Axinte, M.C. Hardy, A.T. Clare, Surface integrity in metal machining — Part II: Functional performance, Int. J. Mach. Tools Manuf. 164 (2021) 103718.
3. Y. Shi, B. Zhao, W. Ding, Solid additives to increase the service life of ceramic cutting tool: Methodology and mechanism, Intell. Sustain. Manuf. 1 (2024) 10009.
4. F. Tavangarian, D. Hui, G. Li, Crack-healing in ceramics, Compos. B Eng. 144 (2018) 56 – 87.
5. P. Greil, Self-healing engineering ceramics with oxidation-induced crack repair, Adv. Eng. Mater. 22 (2020) 1901121.
6. J. Roy, S. Chandra, S. Das, S. Maitra, Oxidation behaviour of silicon carbide-a review, Rev. Adv. Mater. Sci. 38, 1 (2014) 29 – 39.
7. R. Dallaev, Advances in Materials with Self-Healing Properties: A Brief Review, Materials 17, 10 (2024) 2464.
8. X. Cui, Ch. Huang, Zh. Shi, H. Liu, Sh. Li, Y. Han, L. Ji, Zh. Wang, L. Xu, Sh. Huang, The crack-healing and strength recovery mechanisms for the new developed Ti(C,N)-$TiSi_2$-WC composite ceramic tool materials with crack-healing ability, Ceram. Int. 49, 22 (2023) 35382 – 35391.
9. R.H.J. Hannink, P.M. Kelly, B.C. Muddle, Transformation toughening in zirconia-containing ceramics, J. Am. Ceram. Soc. 83 (2000) 461 – 487.
10. N. van Dijk, S. van der Zwaag, Self-healing phenomena in metals, Adv. Mater. Interfaces. 5, 17 (2018) 1800226.
11. K. Laha, J. Kyono, T. Sasaki, S. Kishimoto, N. Shinya, Improved creep strength and creep ductility of type 347 austenitic stainless steel through the self-healing effect of boron for creep cavitation, Metall. Mater. Trans. A 36 (2005) 399 – 409.
12. Y. Fu, C. Kwakernaak, W.G. Sloof, F.D. Tichelaar, E. Brück, S. van der Zwaag, N.H. van Dijk, Competitive healing of creep-induced damage in a ternary Fe-3Au-4W alloy, Metall. Mater. Trans. A 51 (2020) 4442 – 4455.
13. S.B. Luyckx, W. Barlow-Jones, A. Koursaris, N. Mastrantonis, Healing of cracks in WC-Co in the temperature range 600 – 800°C, Int. J. Refract. Met. H. 12, 2 (1993) 89 – 93.
14. A.V. Shatov, S.A. Firstov, I.V. Shatova, The shape of WC crystals in cemented carbides Mater. Sci. Eng. A 242, 1 – 2 (1998) 7 – 14.
15. J. García, V. Collado Ciprés, A. Blomqvist, B. Kaplan, Cemented carbide microstructures: a review, Int. J. Refract. Met. H. 80 (2019) 40 – 68.
16. I. Konyashin, A.A. Zaitsev, D. Sidorenko, E.A. Levashov, B. Ries, S.N. Konischev, M. Sorokin, A.A. Mazilkin, M. Herrmann, A. Kaiser, Wettability of tungsten carbide by liquid binders in WC-Co cemented carbides: Is it complete for all carbon contents, Int. J. Refract. Met. H. 62 (2017) 134 – 148.
17. J. Pittari, J. Swab, J. Wright, K. Atwater, Mechanical evaluation of WC-Co materials with varying microstructures, Int. J. Refract. Met. H. 104 (2022) 105809.
18. R.J. Cao, C.G. Lin, X.C. Xie, Zh. Lin, Microstructure and mechanical properties of WC-Co-based cemented carbide with bimodal WC grain size distribution, Rare Met. 42 (2023) 2809 – 2815.
19. V.I. Stanciu, J.-P. Erauw, L. Boilet, V. Vitry, F. Delaunois, WC-Co composite made with doped binder: The effect of binder proportion on microstructure and mechanical properties, Int. J. Refract. Met. H. 112 (2023) 106161.
20. I.N. Chaporova, K.S. Chernyavsky, Structure of Sintered Hard Alloys, Metallurgy, Moscow, 1975, 248 p. (in Russian)
21. J. Tang, L. Luo, Zh. Liu, X. Zan, Y. Wu, Shape retention of cemented carbide prepared by Co melt infiltration into un-sintered WC green parts made via BJ3DP, Int. J. Refract. Met. H. 107 (2022) 105904.
22. C.L. Cramer, T.G. Aguirre, N.R. Wieber, R.A. Lowden, A.A. Trofimov, H. Wang, J. Yan, M.P. Paranthaman, A.M. Elliott, Binder jet printed WC infiltrated with pre-made melt of WC and Co, Int. J. Refract. Met. H. 87 (2020) 105137.